

# REPORT DOCUMENTATION PAGE

Form Approved  
OMB No. 0704-0188

Public reporting burden for this collection of information is estimated to average 1 hour per response, including the time for reviewing instructions, searching existing data sources, gathering and maintaining the data needed, and completing and reviewing this collection of information. Send comments regarding this burden estimate or any other aspect of this collection of information, including suggestions for reducing this burden to Department of Defense, Washington Headquarters Services, Directorate for Information Operations and Reports (0704-0188), 1215 Jefferson Davis Highway, Suite 1204, Arlington, VA 22202-4302. Respondents should be aware that notwithstanding any other provision of law, no person shall be subject to any penalty for failing to comply with a collection of information if it does not display a currently valid OMB control number. PLEASE DO NOT RETURN YOUR FORM TO THE ABOVE ADDRESS.

1. REPORT DATE (DD-MM-YYYY)		2. REPORT TYPE Technical Papers		3. DATES COVERED (From - To)	
<div style="border: 1px solid black; border-radius: 50%; padding: 20px; text-align: center; font-size: 2em;">                 Please see attached             </div>				4. TITLE AND SUBTITLE	
				5a. CONTRACT NUMBER	
				5b. GRANT NUMBER	
				5c. PROGRAM ELEMENT NUMBER	
				5d. PROJECT NUMBER 2303	
6. AUTHOR(S)				5e. TASK NUMBER M268	
				5f. WORK UNIT NUMBER 345709	
				8. PERFORMING ORGANIZATION REPORT	
7. PERFORMING ORGANIZATION NAME(S) AND ADDRESS(ES) Air Force Research Laboratory (AFMC) AFRL/PRS 5 Pollux Drive Edwards AFB CA 93524-7048				8. PERFORMING ORGANIZATION REPORT	
9. SPONSORING / MONITORING AGENCY NAME(S) AND ADDRESS(ES) Air Force Research Laboratory (AFMC) AFRL/PRS 5 Pollux Drive Edwards AFB CA 93524-7048				10. SPONSOR/MONITOR'S ACRONYM(S)	
12. DISTRIBUTION / AVAILABILITY STATEMENT  Approved for public release; distribution unlimited.				11. SPONSOR/MONITOR'S NUMBER(S) please see attached	
				13. SUPPLEMENTARY NOTES	
14. ABSTRACT  <div style="text-align: right; font-size: 2em; font-weight: bold; border: 1px solid black; padding: 10px; display: inline-block;">20030129 200</div>					
15. SUBJECT TERMS					
16. SECURITY CLASSIFICATION OF:			17. LIMITATION OF ABSTRACT	18. NUMBER OF PAGES	19a. NAME OF RESPONSIBLE PERSON
a. REPORT	b. ABSTRACT	c. THIS PAGE	<div style="border: 1px solid black; border-radius: 50%; width: 40px; height: 40px; margin: 0 auto; display: flex; align-items: center; justify-content: center;"> <span style="font-size: 1.5em;">A</span> </div>		Leilani Richardson
Unclassified	Unclassified	Unclassified			19b. TELEPHONE NUMBER (include area code) (661) 275-5015

MEMORANDUM FOR PRS (In-House Publication)

FROM: PROI (STINFO)

13 Mar 2002

SUBJECT: Authorization for Release of Technical Information, Control Number: AFRL-PR-ED-TP-2002-055  
M. Gerken (Liker Hydrocarbon Rsrch Inst, USC), J. Boatz, K. Christe, et al., "Are <sup>19</sup>F NMR Shifts a Measure for the Nakedness of Fluoride Ions?"

Journal of Flourine Chemistry  
(Deadline: N/A)

(Statement A)

1. This request has been reviewed by the Foreign Disclosure Office for: a.) appropriateness of distribution statement, b.) military/national critical technology, c.) export controls or distribution restrictions, d.) appropriateness for release to a foreign nation, and e.) technical sensitivity and/or economic sensitivity.

Comments: \_\_\_\_\_  
\_\_\_\_\_  
\_\_\_\_\_

Signature \_\_\_\_\_ Date \_\_\_\_\_

2. This request has been reviewed by the Public Affairs Office for: a.) appropriateness for public release and/or b) possible higher headquarters review

Comments: \_\_\_\_\_  
\_\_\_\_\_  
\_\_\_\_\_

Signature \_\_\_\_\_ Date \_\_\_\_\_

3. This request has been reviewed by the STINFO for: a.) changes if approved as amended, b.) appropriateness of distribution statement, c.) military/national critical technology, d.) economic sensitivity, e.) parallel review completed if required, and f.) format and completion of meeting clearance form if required

Comments: \_\_\_\_\_  
\_\_\_\_\_  
\_\_\_\_\_

Signature \_\_\_\_\_ Date \_\_\_\_\_

4. This request has been reviewed by PRS for: a.) technical accuracy, b.) appropriateness for audience, c.) appropriateness of distribution statement, d.) technical sensitivity and economic sensitivity, e.) military/national critical technology, and f.) data rights and patentability

Comments: \_\_\_\_\_  
\_\_\_\_\_  
\_\_\_\_\_

APPROVED/APPROVED AS AMENDED/DISAPPROVED

\_\_\_\_\_  
PHILIP A. KESSEL Date  
Technical Advisor  
Space & Missile Propulsion Division

# ARE $^{19}\text{F}$ NMR SHIFTS A MEASURE FOR THE NAKEDNESS OF FLUORIDE IONS?

M. Gerken,<sup>a</sup> J. A. Boatz,<sup>b</sup> A. Kornath,<sup>a</sup> R. Haiges,<sup>a</sup> S. Schneider,<sup>a</sup> T. Schroer,<sup>a</sup>  
K. O. Christe<sup>a,b\*</sup>

<sup>a</sup>*Loker Hydrocarbon Research Institute and Department of Chemistry, University of Southern California, Los Angeles, California 90089, USA*

<sup>b</sup>*Air Force Research Laboratory, Edwards AFB, California 93524, USA*

Dedicated to Professor David W. A. Sharp, a longtime friend, esteemed colleague and editor of the Journal of Fluorine Chemistry, on the occasion of his retirement.

---

## Abstract

The solvent dependency of the  $^{19}\text{F}$  NMR shifts of the fluoride anion in  $\text{CH}_3\text{OH}$ ,  $\text{H}_2\text{O}$ ,  $\text{CH}_3\text{OCH}_3$ ,  $\text{CHCl}_3$ ,  $\text{CH}_2\text{Cl}_2$ ,  $\text{CHF}_3$ ,  $\text{CH}_3\text{CN}$ ,  $\text{CH}_3\text{NO}_2$ ,  $(\text{CH}_3)_2\text{SO}$ , and  $\text{CH}_3\text{COCH}_3$  solutions was studied by theoretical calculations at the MP2/6-31++G(d,p) and B3LYP/6-31++G(d,p) levels of theory and compared to the experimental values.

It is shown that the free gaseous fluoride anion is most shielded. The stepwise build-up of a solvation sphere was modeled for the  $\text{F}^-/\text{nH}_2\text{O}$  system and results in a progressive deshielding of the  $\text{F}^-$  nucleus with an increasing number of water ligands in the first solvation sphere. Theoretical calculations predict the first solvation sphere of  $\text{F}^-$  to be comprised of six or seven monodentate water molecules. The  $\text{F}\cdots\text{H}$  bond distances increase from 1.42 Å in the monohydrate to 1.69 – 1.87 Å and 1.82 Å in the penta- and hexa-hydrates, respectively, and the transfer of negative charge from  $\text{F}^-$  to the water ligands reaches its maximum for the tetrahydrate.

The wide range of about 70 ppm observed for the chemical shift of  $F^-$  in different solvents and the order of deshielding are confirmed by model calculations involving the interaction between  $F^-$  and a single solvent molecule. Furthermore, it is shown that the deshielding observed for different solvents does not correlate with the calculated binding energies between  $F^-$  and the corresponding solvent molecules, but parallels the increase in the calculated shielding anisotropy in the case of monodentate solvent- $F^-$  adducts. Since the calculated shielding anisotropy for the monodentate adducts can be taken as a qualitative measure for the paramagnetic shielding, the large solvent dependency of the  $F^-$  shifts is best explained by varying amounts of solvent induced paramagnetic shielding. It is also shown that the preferred structure of the  $F^- \cdot CH_3OH$  adduct involves hydrogen bridging through the hydroxyl and not the methyl group and that the minimum energy structures of  $F^- \cdot CH_3SOCH_3$  and  $F^- \cdot CH_3COCH_3$  exhibit bidentate solvent coordination.

In solid fluorides the chemical shift of  $F^-$  spans more than 190 ppm and contrary to intuition an increasing cation size results in increased deshielding of the fluoride anion. As previously shown, this deshielding is due to electronic overlap effects that involve for the larger cations mainly nearest neighbor anion-cation interactions. However for  $Li^+$ , the smallest cation, second neighbor anion-anion overlap becomes also important and causes additional deshielding. The MAS  $^{19}F$ -NMR spectra of solid  $N(CH_3)_4F$  and  $P(CH_3)_4F$  were also measured. The  $F^-$  anion in the  $P(CH_3)_4^+$  salt is 19 ppm less shielded than in the  $N(CH_3)_4^+$  salt in accord with the increased cation size. However in spite of its large size the deshielding caused by the  $N(CH_3)_4^+$  cation is only comparable to that of  $Rb^+$  due to the methyl groups not providing as good an overlap as the smaller but softer  $Cs^+$  cation.

These results show that in both the solid state and in solution the chemical shift of F is not a measure of its nakedness and that the fluoride anion is far from being naked. The only truly naked fluoride anion is the free gaseous fluoride anion.

*Keywords:* Fluoride ion;  $^{19}\text{F}$  NMR shifts; Naked Fluoride; Deshielding; Solvent effects; Solid state effects; Theoretical calculations;  $^{19}\text{F}$ -MAS-NMR spectra of  $\text{N}(\text{CH}_3)_4\text{F}$  and  $\text{P}(\text{CH}_3)_4\text{F}$

---

\*Corresponding author. Tel.: +001-213-7408957; fax: +001-213-7406679.

E-mail address: [kchriste@usc.edu](mailto:kchriste@usc.edu) (K.O. Christe)

## 1. Introduction

Terms such as "naked fluoride ion" or "non-coordinating ion" are frequently and indiscriminately used in spite of the realization that ions in their usual states, i. e., in either solution or the condensed states, are neither naked nor non-coordinating [1-6]. Nevertheless, it is of great general interest to explore methods that allow to measure the extent of nakedness or weakness of coordination. Since the gaseous free fluoride anion is not only naked but also exhibits the highest degree of shielding in its  $^{19}\text{F}$  NMR spectrum (see below), it was interesting to examine whether the degree of deshielding experienced in different environments can serve as a realistic measure for its nakedness.

The  $^{19}\text{F}$  NMR shift of the fluoride anion exhibits a large solvent dependence spanning a range from -73 ppm in  $(\text{CH}_3)_2\text{SO}$  to -148 ppm in  $\text{CH}_3\text{OH}$  solution [7,8]. The shielding of a nucleus can be separated into two main contributions, the diamagnetic shielding and the paramagnetic shielding. The diamagnetic shielding contribution describes the shielding of the nucleus from the external magnetic field by the surrounding electrons that induce a magnetic

field opposite to the external one. The paramagnetic shielding contribution is a perturbation of the electron density currents that generally causes a decrease in the absolute shielding. It is commonly accepted that the  $^{19}\text{F}$  chemical shift is dominated by the paramagnetic shielding term, while the changes in the diamagnetic term are comparatively small [9]. The paramagnetic shielding term vanishes in a spherically symmetric electron distribution thus rendering the gaseous free fluoride ion the most shielded F. A large paramagnetic shielding of fluorine has been correlated with increasing covalency of an F-X bond [9], as exemplified by fluorine chemical shifts for  $\text{CF}_4$  (-63.3 ppm),  $\text{NF}_3$  (146.9 ppm),  $\text{OF}_2$  (250 ppm), and  $\text{F}_2$  (422.9 ppm). Consequently, the  $^{19}\text{F}$  chemical shift could possibly be used as a measure of the "nakedness" of fluoride ions, since a solvent interaction of the fluoride ion should result in an increased polarization of the charge distribution of F leading to an increased paramagnetic shift. However, the large deshielding of F in  $\text{CH}_3\text{CN}$  solution (-74 ppm) when compared with the corresponding value of -119 ppm for an aqueous solution [7] is in marked contrast to the expected weaker solvation.

Previous studies have investigated the correlation between fluoride shielding with hydrogen bonding to the solvent. Miller et al. noted that a correlation between fluoride shielding and hydrogen bonding can only be used with great caution [10]. Symons et al. have shown that chloride ions and atomic xenon exhibit similar solvent dependencies of the  $^{35}\text{Cl}$  and  $^{129}\text{Xe}$  chemical shifts, respectively, compared to  $\delta(^{19}\text{F})$  of fluoride ions. The similar shielding behavior of atomic xenon and the fluoride anion indicates that hydrogen bonding does not dominate the  $^{19}\text{F}$  NMR shift of the fluoride ion in solution [11].

Beside the diamagnetic and paramagnetic shielding terms,  $\sigma_d$  and  $\sigma_p$ , respectively, the shielding of fluoride ions in solution is influenced by van der Waals interactions with the solvent,

$\sigma_w$ , the bulk susceptibility of the solvent,  $\sigma_b$ , magnetic anisotropy of the solvent molecules,  $\sigma_a$ , and solvent electric dipole interactions,  $\sigma_E$ . The shielding contribution from the van der Waals interactions with the solvent has been modeled by Rummens, who developed the reaction field model in order to explain the solvent dependence of  $^{129}\text{Xe}$  chemical shifts of dissolved atomic xenon [12]. His model works quite well for  $^{129}\text{Xe}$  shieldings within homologous series of solvents, like alkanes, cycloalkanes, and alcohols. However, it cannot reproduce shielding trends between solvents of different classes.

Beside the nature of the solvent, the fluoride shielding is influenced to a lesser extent by the fluoride ion concentration and the nature of the counter cation, which have been studied by Tong et al. [13] and Miller et al. [10]. At high fluoride ion concentrations the observed cation effect did not exceed 15 ppm and at infinite dilution, the cation dependence of the  $^{19}\text{F}$  chemical shift was shown to vanish for  $\text{F}^-$  in  $\text{H}_2\text{O}$  and several diols [10].

While in solution and at infinite dilution, the  $^{19}\text{F}$  chemical shift of  $\text{F}^-$  is essentially cation independent and dominated by the nature of the solvent, in the solid state the chemical shift should be dominated by the ion-ion interactions [14-18].

In the present study, the suitability of solution and solid state MAS  $^{19}\text{F}$  NMR spectroscopy for the evaluation of the „nakedness“ of fluoride ions was investigated using both quantum mechanical and experimental methods.

## 2. Results and discussion

### 2.1. Shielding of the free gaseous fluoride anion

The  $^{19}\text{F}$  shielding of the free gaseous fluoride ion was calculated at the MP2/6-31++G(d,p) level [19,20] using the GIAO method [21] and referenced to the calculated value of

+218 ppm for  $\text{CFCl}_3$ . The resulting chemical shift of -260 ppm is 110 ppm more shielded than the most shielded value observed [7] for  $\text{N}(\text{CH}_3)_4\text{F}$  in solution. The paramagnetic shielding term of free gaseous  $\text{F}^-$  is zero due to its spherical charge density. Taking the absolute shielding, i.e., the shielding relative to the bare fluorine nucleus, of  $\text{CFCl}_3$  as 188.7 ppm [22], the fluoride anion has a diamagnetic shielding,  $\sigma_d$ , of 448.7 ppm. However, free gaseous  $\text{F}^-$  does not represent the most shielded fluorine environment, e.g.,  $\text{ClF}$  has a  $^{19}\text{F}$  chemical shift of -419.4 ppm. The extremely high shielding of fluorine in  $\text{ClF}$  has been attributed to a low lying electronic transition which corresponds to electron circulation in opposite senses on the two atoms and results in shielding of fluorine and deshielding of chlorine [23]. The same rationalization has been utilized to explain the surprisingly low  $^{19}\text{F}$  chemical shift for the  $\text{XeF}^+$  cation (-242.5 to -289.8 ppm) compared to its neutral parent molecule  $\text{XeF}_2$  (-181.8 to -199.6 ppm) [24].

## 2.2. Geometries and shielding of solvated fluoride ions

### 2.2.1. Stepwise build-up of the solvation sphere in $\text{F}^- (\text{H}_2\text{O})_n$

The geometries of the adducts formed between the fluoride anion and an increasing number of water molecules were optimized at the MP2/6-31++G(d,p) [19,20] and B3LYP/6-31++G(d,p) [20,25] levels of theory and are shown in Figure 1. It should be noted that in all cases the water molecule acts as a monodentate hydrogen-bridged ligand, in accord with previous relaxation rate measurements [26]. The structures may be qualitatively described as follows: linear H-F-H for the dihydrate, pyramidal  $\text{FH}_3$  for the trihydrate, distorted square planar for the tetrahydrate, square-pyramidal for the pentahydrate, and distorted octahedral for the hexahydrate. Due to the attractive hydrogen bonding interactions between water molecules, the orientation of the water ligands does not adhere to the predictions of the VSEPR model, which assumes repulsive interligand interactions. For instance, VSEPR predicts a trigonal planar

arrangement of the ligands for the trihydrate, in contrast to the observed pyramidal geometry. The latter structure is energetically favored due to the ability of the water ligands to form three intermolecular hydrogen bonds. Several local minima were located for the tetrahydrate,  $F^{\bullet}(H_2O)_4$ . At the MP2/6-31++G(d,p) level, three local minima of  $C_1$ ,  $C_2$ , and  $C_4$  symmetry were found. All three structures have virtually identical energies, with less than 1 kcal/mol separating the highest ( $C_1$ ) and lowest ( $C_4$ ) energy structures. Similarly, at the B3LYP/6-31++G(d,p) level, two local minima of  $C_2$  and  $C_4$  symmetry were found, with a difference in relative energy of less than 1 kcal/mol. The geometries are likewise quite similar, best described as distorted square planar conformations. (Note that only the  $C_2$  geometries are shown in Figure 1.) The  $F^{\bullet}\cdots H$  bond distances increase with an increasing number of water ligands and range from 1.42 Å in the monohydrate to 1.69-1.87 Å and 1.82 Å in the penta- and hexa-hydrates, respectively. As discussed earlier in regard to the structure of  $F^{\bullet}(H_2O)_3$ , the preferred arrangement of the water ligands is influenced both by the  $F^{\bullet}\cdots H$  interaction and hydrogen bonds between water molecules. With the exception of the dihydrate complex, the water ligands tend to agglomerate on one side of  $F^{\bullet}$  (thereby maximizing the number of intermolecular hydrogen bonds) until a sufficient number of water molecules are present to fully encapsulate the anion. This behavior is in contrast to simple VSEPR structural predictions which assume repulsive, rather than attractive (i.e., hydrogen bonding) interligand interactions.

In order to determine (a) the maximum number of water ligands which can directly complex to the fluoride anion (i.e., the size of the first solvation shell) and (b) the effect, if any, of outer solvation shells on the structure of the first solvation shell, additional calculations of the structures of  $F^{\bullet}(H_2O)_n$  ( $n = 7, 8, 12, 20, 49, 86$ ) clusters were performed using the Effective Fragment Potential method [27]. In the EFP approach, the system of interest is divided into

"active" and "spectator" regions. The active region (the fluoride anion in the present case) is treated quantum mechanically while the chemically inert spectator region (the water molecules) is represented by effective fragments which interact with the active component via non-bonded interactions. Although the internal geometry of each fragment water molecule is frozen, the positions of each fragment relative to the fluoride anion and to the other fragments are optimized.

Due to the anticipated large number of energetically similar local minima, approximate stationary points were initially located using Monte Carlo random sampling methods [28] and were subsequently refined using conventional gradient-based optimization methods. All stationary points found in this manner were confirmed as local minima via diagonalization of the energy second derivative matrix (i.e., the hessian matrix) to verify the presence of all real harmonic vibrational frequencies. All EFP calculations were performed at the RHF level, using the Dunning and Hay basis set augmented with polarization functions and a diffuse s+p shell on oxygen and fluorine (denoted as DH+(d,p)) [29].

A more detailed analysis of the EFP/DH+(d,p) structures of the  $F^-(H_2O)_n$  ( $n = 7, 8, 12, 20, 49, 86$ ) clusters will be reported elsewhere [30]; here we simply report that the first solvation shell typically is found to consist of seven water molecules arranged in an approximate pentagonal bipyramidal geometry around the fluoride anion, with the F...H bond lengths ranging from 1.84 to 2.34 Å. In the case of the  $F^-(H_2O)_{20}$  cluster, the first solvation shell was found to contain an approximately octahedral arrangement of six water molecules about the central fluoride anion, with F...H bond lengths ranging from 1.84 to 1.89 angstroms. Therefore, the first solvation shell is predicted to contain at most seven water molecules, with all additional water molecules residing in outer solvation spheres. However, due to the vast number of possible local minima, there is no guarantee that the optimized structures obtained here are in fact the global

minima. Therefore, these results should be regarded as merely suggestive rather than definitive predictions of the structure of the first solvation shell.

The extent of negative charge transfer from  $F^-$  to the water ligands was calculated using the Natural Population Analysis (NPA) [31] and Löwdin's population analysis [32] methods. Charge transfer from  $F^-$  to the surrounding water molecules is maximized at  $F^- \cdot 4H_2O$  (see Figure 2). Clearly, the amount of charge transfer is governed not only by the number of ligands but also by the  $F \cdots H$  bond distances which increase with an increasing number of ligands.

The  $^{19}F$  chemical shifts were calculated using the GIAO method [21] and are summarized in Table 1 and Figure 3. Although the trends in Figures 2 and 3 are similar, a plot of the chemical shifts against the atomic charge on fluorine (Figure 4) does not result in a straight line but exhibits significant curvature indicating that the chemical shift is not totally dependent upon the extent of charge transfer. The chemical shift of about  $-136$  ppm calculated at the MP2 level for a complete first solvation sphere is in fair agreement with the observed value of  $-119$  ppm for an aqueous solution [7], particularly if one keeps in mind the neglect of the outer solvation spheres.

#### 2.2.2. Solvent dependence of the chemical shift of $F^-$

The geometries of adducts between fluoride and one solvent molecule of  $H_2O$ ,  $(CH_3)_2SO$ ,  $(CH_3)_2CO$ ,  $CH_3CN$ ,  $CH_3NO_2$ ,  $CH_3OCH_3$ ,  $CH_3OH$ ,  $CHF_3$ ,  $CHCl_3$ , and  $CH_2Cl_2$  were optimized at the MP2/6-31++G(d,p) level of theory, and the structural parameters are summarized in Figures 1 and 5. For  $CH_3OH$  where fluorine bridging could occur through either the hydroxyl or the methyl group, the hydroxyl-bridged structure was found to be energetically favored by 20.8 kcal/mol. In the cases of  $CH_3CN$  and  $CH_3NO_2$ , the energetically favored bridging mode involves one of the hydrogen atoms of the methyl groups. In compounds containing only one methyl group, monodentate bridging was always favored over multidentate bridging and is in accord

with the preference for monodentate bridging of water. In the two compounds containing two methyl groups and either an S=O or C=O bridge, the oxygen atoms force two hydrogens from different methyl groups into positions favoring bidentate minimum energy structures. These structures differ from those of the monodentate ones but their chemical shifts are predicted equally well by the theoretical calculations (see below). In  $\text{CH}_3\text{OCH}_3$  the methyl hydrogens are further apart and monodentate bridging is favored. The  $^{19}\text{F}$  NMR shifts of these adducts were also calculated by the GIAO method [21] and are given in Table 2.

The calculated  $^{19}\text{F}$  chemical shifts of these mono-adducts are  $76 \pm 9$  ppm lower than the observed ones [7-9] which is in fair agreement with the calculated difference of -67 ppm between the monohydrate and the hexahydrate (see above), particularly if the neglect of secondary solvation effects is kept in mind. The only exception was the previously reported chemical shift for F<sup>-</sup> in  $\text{CH}_3\text{NO}_2$  solvent (-150 ppm) [7] which was inconsistent with the calculated chemical shift after correction for full solvation (-67 ppm). An NMR spectroscopic reinvestigation of  $\text{N}(\text{CH}_3)_4\text{F}$  in  $\text{CH}_3\text{NO}_2$  solution at temperatures close to the freezing point of the solvent (at -25 °C) showed only a doublet at -147.5 ppm in the  $^{19}\text{F}$  and a triplet at 17.0 ppm in the  $^1\text{H}$  NMR spectrum ( $^1J(^1\text{H}-^{19}\text{F}) = 121$  Hz) due to the  $\text{HF}_2^-$  anion. No evidence was found for free fluoride indicating an immediate attack of  $\text{CH}_3\text{NO}_2$  by F<sup>-</sup> even at low temperature rendering the previous assignment of the  $^{19}\text{F}$  NMR resonance at -150 ppm to F<sup>-</sup> erroneous.

Our simplified theoretical model of a gaseous fluoride anion with only one solvent molecule, confirms the chemical shifts observed for the fully solvated ions, their wide shift range, and the solvent orders. Furthermore, secondary effects must be minor, and the observed shifts must correlate with properties that are derivable from the ab initio and isotropic shielding

calculations. The decrease in the calculated shielding for the monodentate solvent F<sup>-</sup> adducts is paralleled by an increase in the calculated shielding anisotropy,  $\Delta\sigma$ , which is defined by eq. (1),

$$\Delta\sigma = \sigma_{33} - (\sigma_{22} + \sigma_{11})/2 \quad (1)$$

(with  $\sigma_{33} \geq \sigma_{22} \geq \sigma_{11}$ )

where  $\sigma_{33}$ ,  $\sigma_{22}$ , and  $\sigma_{11}$  are the diagonal components of the shielding tensor in the principle axis system in which all off-diagonal elements of the shielding tensor are zero. Since in the monodentate  $\text{CHCl}_3$  and  $\text{CHF}_3$  adducts the shielding is axially symmetric and in the  $\text{H}_2\text{O}$ ,  $\text{CH}_3\text{CN}$ ,  $\text{CH}_3\text{NO}_2$ ,  $\text{CH}_3\text{OCH}_3$ ,  $\text{CH}_3\text{OH}$ , and  $\text{CH}_2\text{Cl}_2$  adducts it is approximately axially symmetric, the shielding anisotropy can be taken as a crude, qualitative measure for the size of the paramagnetic shielding. However,  $\Delta\sigma$  provides a quantitative measure of the paramagnetic shielding only for linear molecules, in which the paramagnetic shielding component parallel to the molecular axis,  $\sigma_{\parallel}^{\text{P}}$ , is zero [33]. For  $^{19}\text{F}$  in the monodentate F<sup>-</sup> adducts, the largest calculated shielding components in the principle axis system ( $\sigma_{33}$ ), which corresponds to the  $\sigma_{\parallel}$  component in linear molecules, deviate only slightly ( $\pm 11$  ppm) from the diamagnetic shielding of 478 ppm found for free gaseous F<sup>-</sup>. This indicates a negligible paramagnetic contribution to  $\sigma_{33}$  and supports the validity of the qualitative correlation of  $\Delta\sigma$  and  $\sigma^{\text{P}}$ . Therefore, the large solvent dependency of the F<sup>-</sup> shifts is best explained by varying amounts of solvent induced paramagnetic shielding.

The binding energies of the mono-adducts of F<sup>-</sup> with the different solvent molecules were calculated at the MP2/6-31++G(d,p) [19,20] and CCSD(T)/6-311++G(d,p)//MP2/6-31++G(d,p) [20,34,35] levels of theory and are included in Table 2. The calculated binding energies correlate well, as expected, with the calculated F<sup>-</sup>...H bond distances, but show no correlation with the observed  $^{19}\text{F}$  chemical shifts. The influence of the bulk susceptibility on the

$^{19}\text{F}$  chemical shift was not included in the shift calculations, and is not expected to play a dominating role in the solvent dependence of the  $^{19}\text{F}$  chemical shift of the fluoride ion [36].

### 2.3. Chemical shielding in the solid state

All alkali metal fluorides are face-centered cubic. If these salts were completely ionic and there were no ion-ion interactions, the fluoride ions should be isotropic, there should be no paramagnetic contributions to the shielding, and the diamagnetic shielding of the  $\text{F}^-$  ion should be comparable in all salts and approximate that of the free ion. In reality, the chemical shifts observed for the solid alkali metal fluorides are strongly deshielded and span more than 200 ppm, indicating significant paramagnetic contributions that are cation dependent (see Table 3). Although the solid state  $^{19}\text{F}$  NMR spectra of the alkali metal fluorides have been the subject of numerous experimental [18,37-40] and theoretical [14-18,37,38,41-43] studies, it was interesting to obtain experimental data for the noncubic  $\text{N}(\text{CH}_3)_4\text{F}$  and  $\text{P}(\text{CH}_3)_4\text{F}$  salts. The  $\text{N}(\text{CH}_3)_4\text{F}$  salt is hexagonal [7] and its  $\text{F}^-$  anion is octahedrally surrounded by six  $\text{N}(\text{CH}_3)_4^+$  cations with an anion-cation separation of  $R = 3.80 \text{ \AA}$ .

The solid state  $^{19}\text{F}$  MAS NMR spectra of  $\text{N}(\text{CH}_3)_4\text{F}$  and  $\text{P}(\text{CH}_3)_4\text{F}$  were recorded and are given in Figure 6 and Table 3, together with those of  $\text{KF}$  and  $\text{RbF}$  and literature values for  $\text{LiF}$ ,  $\text{NaF}$ , and  $\text{CsF}$  [18]. Our  $^{19}\text{F}$  chemical shifts of  $-132$  and  $-91$  ppm for  $\text{KF}$  and  $\text{RbF}$ , respectively, agree well with those previously reported [18,37,38]. The alkali metal fluorides, excluding  $\text{LiF}$ , show a decrease in shielding with increasing cation radius. The same trend has been observed for the  $^{35}\text{Cl}$ ,  $^{79}\text{Br}$ , and  $^{127}\text{I}$  NMR shifts of alkali metal chlorides, bromides, and iodides [18]. On first sight, this trend is counter-intuitive, since the  $^{19}\text{F}$  chemical shift of these isostructural fluorides should be determined mainly by the cation-anion interactions and the largest cation should give rise to the most naked fluoride, i.e., the fluoride with the highest shielding. However, Kondo and

Yamashita have successfully correlated the observed chemical shifts in the alkali metal halides with the increasing overlap between the nearest neighbors, i. e., the halide anions and the alkali metal cations, resulting from the increasing cation size. The fact that the smallest alkali metals do not follow the general trend has been attributed to the small size of these cations, resulting in second nearest neighbor contacts, i. e., anion-anion overlap that causes additional deshielding [15]. The observed trends in the  $^{19}\text{F}$  NMR shifts have recently been matched well by density functional calculations for the LiF, NaF, KF, RbF series and correlated with the ion-ion repulsive energy term,  $-Q_+Q_-/R^2$ , where R represents the shortest anion-cation distance in the crystal lattice and  $Q_+$  and  $Q_-$  are the ionic charges [42,43]. However, the observed shift of CsF does not fit this correlation and the values of 0.7, 1.0, 1.0, and 1.0, assumed for the ionic charges of LiF, NaF, KF, and RbF, respectively, are not in accord with the generally assumed values of 0.74, 0.75, 0.84, and 0.86 for the ionicity of these alkali metal fluorides [44]. When the latter values for the ionicities are used, the correlation with the ion-ion repulsive energy term becomes very poor, indicating the need for a better correlation.

Tetramethyl ammonium fluoride and  $\text{P}(\text{CH}_3)_4\text{F}$  have  $^{19}\text{F}$  chemical shifts of  $-91$  and  $-72$  ppm, respectively, that are close to that of RbF. While  $\text{N}(\text{CH}_3)_4\text{F}$  is an ionic compound that crystallizes in the hexagonal system [7],  $\text{P}(\text{CH}_3)_4\text{F}$  has been shown to exist as a covalent compound in the gas phase with pentacoordinate phosphorus [45]. However, in the solid state  $\text{P}(\text{CH}_3)_4\text{F}$  exhibits an ionic structure [45] and, therefore, its solid state  $^{19}\text{F}$  NMR shift can be compared to that of the tetramethyl ammonium salt. Although the sizes of the  $\text{N}(\text{CH}_3)_4^+$  and  $\text{P}(\text{CH}_3)_4^+$  cations are considerably larger than that of  $\text{Cs}^+$ , the fluoride anions in these salts are less deshielded. This can be attributed to the lower polarizability of the methyl groups when compared to the much softer alkali metal cations resulting in less overlap. The fact that the F

anion in  $\text{P}(\text{CH}_3)_4\text{F}$  is 19 ppm more deshielded than that in  $\text{N}(\text{CH}_3)_4\text{F}$  can be attributed to the larger size of the  $\text{P}(\text{CH}_3)_4^+$  cation.

### 3. Experimental

The preparations of  $\text{N}(\text{CH}_3)_4\text{F}$  [7] and  $\text{P}(\text{CH}_3)_4\text{F}$  [45] have previously been described. The  $\text{KF}$  and  $\text{RbF}$  were dried by fusion in a platinum crucible. The hot clinkers were immediately transferred to the dry nitrogen atmosphere of a glove box which was also used for loading the  $^{19}\text{F}$  MAS NMR rotors.

Theoretical Methods: The geometries of  $\text{F}\cdot(\text{H}_2\text{O})_n$  ( $n = 1-6$ ) and  $\text{F}\cdot\text{S}$  ( $\text{S} = (\text{CH}_3)_2\text{SO}$ ,  $(\text{CH}_3)_2\text{CO}$ ,  $\text{CH}_3\text{CN}$ ,  $\text{CH}_3\text{NO}_2$ ,  $\text{CH}_3\text{OCH}_3$ ,  $\text{CH}_3\text{OH}$ ,  $\text{CHF}_3$ ,  $\text{CHCl}_3$ , and  $\text{CH}_2\text{Cl}_2$ ) were fully optimized at the MP2/6-31++G(d,p) level [19,20]. The  $\text{F}\cdot(\text{H}_2\text{O})_n$  clusters were also optimized using density functional theory methods, at the B3LYP/6-31++G(d,p) level [20,25]. Each structure was verified as a local minimum via diagonalization of the matrix of energy second derivatives with respect to nuclear coordinates (i.e., the hessian matrix). Atomic charges were computed using the Natural Population Analysis (NPA) [31] and Löwdin's population analysis [32] methods. Binding energies of each single-molecule adduct with  $\text{F}$  were computed at the CCSD(T) [34] level using the 6-311++G(d,p) [46-48] basis set. The geometries of the larger water clusters  $\text{F}\cdot(\text{H}_2\text{O})_n$  ( $n = 7,8,12,20,49,86$ ) were optimized at the RHF/DH+(d,p) level [29] using the Effective Fragment Potential (EFP) method [27]. All calculations were performed using GAMESS [49], Gaussian98 [50], and ACESII [51].

#### 4. Conclusions

The above study shows that  $^{19}\text{F}$  NMR shifts are not a measure for the nakedness of the fluoride anion. This applies to both solution and solid state spectra. In solution, the chemical shift of the fluoride anion is strongly influenced by solvent induced paramagnetic shielding, while in the solid state the deshielding is governed by electronic overlap effects involving mainly nearest neighbour, anion-cation, interactions, except for the cases where one ion is much smaller than the other and second-nearest neighbor, anion-anion or cation-cation, interactions become also important. Furthermore, it is shown that both in solution and in the solid state a truly naked fluoride ion does not exist and that the gaseous free fluoride ion is the only naked fluoride ion.

Simplified model calculations at the MP2 level involving adducts between the free fluoride anion and only one solvent molecule were successfully used to reproduce the observed solvent shifts and to explain the nature of the deshielding. Furthermore, the stepwise build-up of the water solvent sphere was modeled showing that the first solvent sphere of  $\text{F}^-$  contains a maximum of 6-7 water molecules.

The MAS  $^{19}\text{F}$  NMR spectra of  $\text{N}(\text{CH}_3)_4\text{F}$  and  $\text{P}(\text{CH}_3)_4\text{F}$  were measured and compared to those of the alkali metal fluorides. It is shown that the ion size is not the only factor determining the deshielding of  $\text{F}^-$  in these two salts and that other effects, such as the polarizability of the cations, may also play a significant role in influencing the ion-ion overlap.

#### Acknowledgements

The authors thank Prof. James Haw for the recording of the MAS  $^{19}\text{F}$  NMR spectra. The National Science Foundation has financially supported the work at USC and the Air Force Office

of Scientific Research that at Edwards. One of us (M.G.) is grateful to the National Sciences and Engineering Research Council of Canada for a postdoctoral fellowship. This work was also supported in part by grants of Cray T916 time and IBM SP time at the Department of Defense High Performance Computing Modernization Program Major Shared Resource Centers located at the Army Research Laboratory (Aberdeen Proving Ground) and the Aeronautical Systems Center (Wright-Patterson AFB).

## References

- [1] K. Seppelt, *Angew. Chem., Int. Ed. Engl.* 31 (1992) 292-293.
- [2] B. K. Bennett, R. G. Harrison, T. G. Richmond, *J. Am. Chem. Soc.* 116 (1994) 11165-11166.
- [3] V. V. Grushin, *Angew. Chem., Int. Ed. Engl.* 37 (1998) 994-996.
- [4] R. D. Chambers, W. K. Gray, G. Sanford, J. F. S. Vaughan, *J. Fluorine Chem.* 94 (1999) 213-215.
- [5] P. K. Hurlburt, D. M. Van Seggen, J. J. Rack, S. H. Strauss, in J. S. Thrasher, S. H. Strauss (Eds.), *Inorganic Fluorine Chemistry*, ACS Symposium Series 555, American Chemical Society, Washington DC, 1994, pp. 338-349.
- [6] K. Seppelt, *Angew. Chem., Int. Ed. Engl.* 32 (1993) 1025-1027 and references cited therein.
- [7] K. O. Christe, W. W. Wilson, R. D. Wilson, R. Bau, J. Feng, *J. Am. Chem. Soc.* 112 (1990) 7619-7625.
- [8] K. O. Christe, W. W. Wilson, *J. Fluorine Chem.* 46 (1990) 339-342.
- [9] S. Berger, S. Braun, H.-O. Kalinowski (Eds.), *NMR-Spektroskopie von Nichtmetallen*, Bd. 4, <sup>19</sup>F-NMR Spectroskopie, Georg Thieme Verlag, Stuttgart, 1994, pp. 2,3.

- [10] J. M. Miller, R. K. Kanippayoor, J. H. Clark, *J. Chem. Soc., Dalton Trans.* (1983) 683-687.
- [11] C. Carmona, G. Eaton, M. C. R. Symons, *J. Chem. Soc., Chem. Commun.* (1987) 873-874.
- [12] F. H. A. Rummens, *NMR Basic Principles and Progress* 10 (1975) 1-118; C. I. Ratcliffe  
*Ann. Rep. NMR Spectrosc.* 36(1998) 123-221.
- [13] J. P. K. Tong, C. H. Langford, T. R. Stengle, *Can. J. Chem.* 52 (1974) 1721-1731.
- [14] K. Yoshida, T. Moriya, *J. Phys. Soc. Jpn.* 11 (1956) 33-49.
- [15] J. Kondo, J. Yamashita, *J. Phys. Chem. Solids* 10 (1959) 245-253.
- [16] R. Baron, *J. Chem. Phys.* 38 (1963) 173-187.
- [17] Y. Yamagata, *J. Phys. Soc. Jpn.* 19 (1964) 10-23.
- [18] S. Hayashi, K. Hayamizu, *Bull. Chem. Soc. Jpn.* 63 (1990) 913-919.
- [19] R. J. Bartlett, D. M. Silver, *Int. J. Quantum Chem.* S9 (1975) 183; J. A. Pople, J. S.  
Binkley, R. Seeger, *Int. J. Quantum Chem.* S10 (1976) 1-19; M. J. Frisch, M. Head-Gordon, J.  
A. Pople, *Chem. Phys. Lett.* 166 (1990) 275-280.
- [20] R. Ditchfield, W. J. Hehre, J. A. Pople, *J. Chem. Phys.* 54 (1971) 724-728; W. J. Hehre, R.  
Ditchfield, J. A. Pople, *J. Chem. Phys.* 56 (1972) 2257-2261; M. M. Francl, W. J. Pietro, W. J.  
Hehre, J. S. Binkley, M. S. Gordon, D. J. DeFrees, J. A. Pople, *J. Chem. Phys.* 77 (1982) 3654-  
3665.
- [21] J. Gauss, *Chem. Phys. Lett.* 191 (1992) 614; J. Gauss, *J. Chem. Phys.* 99 (1993) 3629.
- [22] D. K. Hindemann, C. D. Cornwell, *J. Chem. Phys.* 48 (1968) 4148-4154; *J. Chem. Phys.* 48  
(1968) 2017-2025.
- [23] C. D. Cornwell, *J. Chem. Phys.* 44 (1966) 874-880.
- [24] M. Gerken, G. J. Schrobilgen, *Coord. Chem. Rev.* 197 (2000) 335-395.

- [25] A. D. Becke, *J. Chem. Phys.* **98** (1993) 5648-5642; P. J. Stephens, F. J. Devlin, C. F. Chablowski, M. J. Frisch, *J. Phys. Chem.* **98** (1994) 11623-11627; R. H. Hertwig, W. Koch, *Chem. Phys. Lett.* **268** (1997) 345-351.
- [26] H. G. Hertz, C. Rädle, *Ber. Bunsenges. Phys. Chem.* **77** (1973) 521-531.
- [27] See, for example, M.S. Gordon, M.A. Freitag, P. Bandyopadhyay, V. Kairys, J. H. Jensen, W. J. Stevens, *J. Phys. Chem. A*, **105**, (2001) 293; P. N. Day, J. H. Jensen, M. S. Gordon, S. P. Webb, W. J. Stevens, M. Krauss, D. Garmer, H. Basch, D. Cohen, *J. Chem. Phys.*, **105** (1996) 1968.
- [28] See, for example, P. N. Day, R. Pachter, M. S. Gordon and G. N. Merrill, *J. Chem. Phys.*, **112** (200) 2063.
- [29] T. H. Dunning, Jr., P. J. Hay. Chapter 1 in "Methods of Electronic Structure Theory", H. F. Shaefer III, Ed. Plenum Press, N.Y. 1977, pp 1-27. Inner and outer scale factors of 1.2 and 1.15, respectively, were used for hydrogen. Exponents of the d polarization functions for fluorine and oxygen are 0.90 and 0.85, respectively. The exponent of the p polarization function on hydrogen is 1.0.
- [30] K. O. Christe, J. A. Boatz, manuscript in preparation.
- [31] A. E. Reed, R. B. Weinstock, F. A. Weinhold, *J. Chem. Phys.* **83** (1985) 735-746; A. E. Reed, L. A. Curtiss, F. Weinhold, *Chem. Rev.* **88** (1988) 899-926.
- [32] P.-O. Löwdin, *Adv. Chem. Phys.* **5** (1970) 185-199.
- [33] C. J. Jameson, Chemical Shift Scales on an Absolute Basis, In *The Encyclopedia of Nuclear Magnetic Resonance*, D. M. Grant, R. K. Harris (Eds.), New York: John Wiley and Sons, 1996, pp. 1273-1281.

- [34] K. Raghavachari, G. W. Trucks, J. A. Pople, M. Head-Gordon, *Chem. Phys. Lett.* 157 (1989) 479; R. J. Bartlett, J. D. Watts, S. A. Kucharski, J. Noga, *Chem. Phys. Lett.* 165 (1990) 513; J. Gauss, W. J. Lauderdale, J. F. Stanton, J. D. Watts, R. J. Bartlett, *Chem. Phys. Lett.* 182(1991) 207; J. D. Watts, J. Gauss, R. J. Bartlett, *J. Chem. Phys.* 98 (1993) 8718.
- [35] The notation „MethodA/BasisA//MethodB/BasisB“ denotes single-point energy calculations at the MethodA/BasisA level using geometries optimized at the MethodB/BasisB level.
- [36] C. J. Jameson, J. Mason, in J. Mason (Ed.), *Multinuclear NMR*, Plenum Press, New York and London, 1987, Chapter 2, p 42.
- [37] A. T. Kreinbrink, C. D. Sazavsky, J. W. Pyrz, D. G. A. Nelson, R. S. Honkonen, *J. Magn. Res.* 88 (1990) 267-276.
- [38] J. M. Miller, *Progr. Nucl. Magn. Reson. Spectr.* 28 (1996) 255-281, and references cited therein.
- [39] R. E. J. Sears, *J. Chem. Phys.* 61 (1974) 4368.
- [40] R. K. Harris, P. Jackson, *Chem. Rev.* 91 (1991) 1427.
- [41] M. Mortimer, E. A. Moore, N. F. Peirson, *J. Chem. Soc., Faraday Trans.* 92 (1992) 1117.
- [42] S. H. Cai, Z. Chen, X. Xu, H. L. Wan, *Chem. Phys. Lett.* 302 (1999) 73.
- [43] S. H. Cai, Z. Chen, H. L. Wan, *J. Phys. Chem.* 106 (2002) 1060.
- [44] R. T. Sanderson, in *Chemical Bonds and Bond Energy, Physical Chemistry, A Series of Monographs*, Vol. 21, Academic Press, New York, second ed. 1976, p 153.
- [45] A. Kornath, F. Neumann, H. Oberhammer, to be published.
- [46] R. Krishnan, J. S. Binkley, R. Seeger, J. A. Pople, *J. Chem. Phys.* 72 (1980) 650-654.
- [47] P. C. Hariharan, J. A. Pople, *Theoret.Chim.Acta* 28 (1973) 213-222.

- [48] T. Clark, J. Chandrasekhar, G. W. Spitznagel, P. von R. Schleyer *J. Comput. Chem.* 4 (1983) 294-301; M. J. Frisch, J. A. Pople, J. S. Binkley, *J. Chem. Phys.* 80 (1984) 3265-3269.
- [49] M. W. Schmidt, K. K. Baldrige, J. A. Boatz, S. T. Elbert, M. S. Gordon, J. J. Jensen, S. Koseki, N. Matsunaga, K. A. Nguyen, S. Su, T. L. Windus, M. Dupuis, J. A. Montgomery, *J. Comput. Chem.* 14 (1993) 1347-1363.
- [50] Gaussian 98, Revision A.7, M. J. Frisch, G. W. Trucks, H. B. Schlegel, G. E. Scuseria, M. A. Robb, J. R. Cheeseman, V. G. Zakrzewski, J. A. Montgomery, Jr., R. E. Stratmann, J. C. Burant, S. Dapprich, J. M. Millam, A. D. Daniels, K. N. Kudin, M. C. Strain, O. Farkas, J. Tomasi, V. Barone, M. Cossi, R. Cammi, B. Mennucci, C. Pomelli, C. Adamo, S. Clifford, J. Ochterski, G. A. Petersson, P. Y. Ayala, Q. Cui, K. Morokuma, D. K. Malick, A. D. Rabuck, K. Raghavachari, J. B. Foresman, J. Cioslowski, J. V. Ortiz, A. G. Baboul, B. B. Stefanov, G. Liu, A. Liashenko, P. Piskorz, I. Komaromi, R. Gomperts, R. L. Martin, D. J. Fox, T. Keith, M. A. Al-Laham, C. Y. Peng, A. Nanayakkara, C. Gonzalez, M. Challacombe, P. M. W. Gill, B. Johnson, W. Chen, M. W. Wong, J. L. Andres, C. Gonzalez, M. Head-Gordon, E. S. Replogle, J. A. Pople, Gaussian, Inc., Pittsburgh PA, 1998.
- [51] ACESII is a program product of the Quantum Theory Project, University of Florida. Authors: J. F. Stanton, J. Gauss, J. D. Watts, M. Nooijen, N. Oliphant, S. A. Perera, P. G. Szalay, W. J. Lauderdale, S. R. Gwaltney, S. Beck, A. Balkova, D. E. Bernholdt, K. -K. Baeck, P. Rozyczko, H. Sekino, C. Huber, R. J. Bartlett. Integral Packages: VMOL (J. Almlöf, P. R. Taylor); VPROPS (P. R. Taylor); ABACUS (T. Helgaker, H. J. Aa. Jensen, P. Jorgenson, J. Olsen, P. R. Taylor).

Table 1

Calculated (MP2)  $^{19}\text{F}$  chemical shifts of the free fluoride ion and its water adducts.

	$\delta(^{19}\text{F})$ , ppm
F	-260.0
F(H <sub>2</sub> O)	-203.4
F(H <sub>2</sub> O) <sub>2</sub>	-181.0
F(H <sub>2</sub> O) <sub>3</sub>	-162.8
F(H <sub>2</sub> O) <sub>4</sub>	-148.9
F(H <sub>2</sub> O) <sub>5</sub>	-142.3
F(H <sub>2</sub> O) <sub>6</sub>	-135.9

Table 2

Observed and calculated MP2  $^{19}\text{F}$  chemical shifts, calculated shielding anisotropies ( $\Delta\sigma$ ), binding energies, and  $\text{F}\cdots\text{H}$  bond distances of the fluoride anion in different solvents.

	$\delta(^{19}\text{F})$ , ppm			$\Delta\sigma$ , ppm	F(X) Binding energy, kcal/mol		$r_{\text{F}\cdots\text{H}}$ , Å
	$\delta$ calcd. for monosolvate <sup>a</sup>	calcd. $\delta$ corrected for full solvation <sup>b</sup>	$\delta$ obsd. for solutions of $[\text{N}(\text{CH}_3)_4][\text{F}]^{\text{c}}$		calcd. <sup>d</sup>	calcd.	
<b>F (free gaseous ion)</b>	-260						
<b>Monodentate</b>							
F(HOCH <sub>3</sub> )	-215.3	-140.5	-148	71.7	29.1(29.8)	1.374	
F(CH <sub>3</sub> OH) <sup>e</sup>	(-212.6)	-	-		-	-	
F(CH <sub>3</sub> OCH <sub>3</sub> )	-207.7	-132.9	- <sup>f</sup>	93.1	9.0(9.7)	1.872	
F(H <sub>2</sub> O)	-203.4	-128.6	-119	92.7	27.4(27.5)	1.415	
F(CHCl <sub>3</sub> )	-186.8	-112.0	-113	94.5	31.1(32.2)	1.377	
F(CH <sub>2</sub> Cl <sub>2</sub> )	-182.4	-107.6	-109	112.9	23.7(24.5)	1.544	
F(CHF <sub>3</sub> )	-169.9	-94.8	-107	120.9	27.7(27.9)	1.536	
F(CH <sub>3</sub> CN)	-153.1	-78.3	-74	176.4	22.1(23.2)	1.571	
F(CH <sub>3</sub> NO <sub>2</sub> )	-134.8	-60.0	- <sup>g</sup>	192.4	25.7(27.1)	1.449	
<b>Bidentate</b>							
F(CH <sub>3</sub> COCH <sub>3</sub> )	-184.8	-110.0	-103	72.3	21.2(21.8)	1.962	
F((CH <sub>3</sub> ) <sub>2</sub> SO)	-157.2	-82.4	-73	89.5	29.7(30.4)	1.876	

<sup>a</sup> Obtained by subtraction of the calculated isotropic shielding of the F monosolvates from that of  $\text{CFCl}_3$  (+217.9 ppm.)

<sup>b</sup> An empirical correction of 74.8 ppm was applied to give the best fit with the observed data.

<sup>c</sup> Values taken from ref [7] except for the value for  $\text{CH}_2\text{Cl}_2$  that was taken from refs [2,3].

<sup>d</sup> CCSD(T)/6-311++G(d,p)//MP2/6-31++G(d,p) binding energies are given in parentheses.

<sup>e</sup> Less stable than the hydroxyl bridged isomer by 20.8 kcal/mol.

<sup>f</sup> Not observed due to low solubility.

<sup>g</sup> The previously reported chemical shift of -150 ppm was found to be erroneous and has to be attributed to the  $\text{HF}_2^-$  anion. Tetramethylammonium fluoride reacts with  $\text{CH}_3\text{NO}_2$  even at -25 °C; thus, no experimental  $\delta(^{19}\text{F})$  for fluoride in  $\text{CH}_3\text{NO}_2$  could be obtained.

Table 3

Observed solid state  $^{19}\text{F}$  chemical shifts for various fluorides.

	$\delta(^{19}\text{F}), \text{ppm}$
LiF	-204 <sup>a</sup>
NaF	-221 <sup>a</sup>
KF	-132 <sup>b</sup>
RbF	-91 <sup>b</sup>
CsF	-8 <sup>a</sup>
$[\text{N}(\text{CH}_3)_4][\text{F}]$	-91 <sup>b</sup>
$[\text{P}(\text{CH}_3)_4][\text{F}]$	-72 <sup>b</sup>

<sup>a</sup> Values from ref [18].

<sup>b</sup> Values from this study.

**Diagram Captions:**

**Fig. 1.** Stepwise build-up of the hydration sphere of the fluoride anion. Minimum energy structures of the free mono- to hexa-hydrates of the fluoride anion at the MP2/6-31++G(d,p) and B3LYP/6-31++G(d,p) (in parentheses) levels.

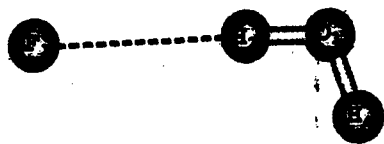
**Fig. 2.** Plot of the calculated NPA and Löwdin atomic charges on fluorine as a function of the number of water ligands during the stepwise build-up of the fluoride anion hydration sphere.

**Fig. 3.** Plot of the calculated  $^{19}\text{F}$  NMR shifts against the number of water ligands in the stepwise build-up of the hydration sphere of the fluoride anion.

**Fig. 4.** Plot of the calculated  $^{19}\text{F}$  NMR shifts against the nuclear charge transfer from the fluoride ion to the water ligands during the stepwise build-up of the hydration sphere of the fluoride anion.

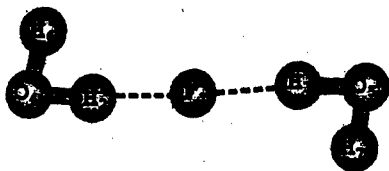
**Fig. 5.** MP2/6-31++G(d,p) calculated structural parameters for adducts between fluoride and one molecule of  $\text{CH}_3\text{SOCH}_3$ ,  $\text{CH}_3\text{COCH}_3$ ,  $\text{CH}_2\text{Cl}_2$ ,  $\text{CH}_3\text{OH}$ ,  $\text{CH}_3\text{OCH}_3$ ,  $\text{CH}_3\text{NO}_2$ ,  $\text{CHCl}_3$ ,  $\text{CHF}_3$ , and  $\text{CH}_3\text{CN}$ .

**Fig. 6.** Observed MAS  $^{19}\text{F}$  NMR spectra of  $\text{P}(\text{CH}_3)_4\text{F}$ ,  $\text{RbF}$ ,  $\text{N}(\text{CH}_3)_4\text{F}$ , and  $\text{KF}$ .



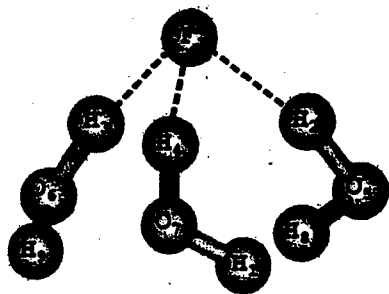
$C_{2v}$

F1-H2	1.415(1.385)
H2-O3	1.051(1.066)
O3-H4	0.963(0.964)
F1-H2-O3	174.9(175.4)
H2-O3-H4	102.4(102.8)
$\omega$ (F1-H2-O3-H4)	0.0( 0.0)



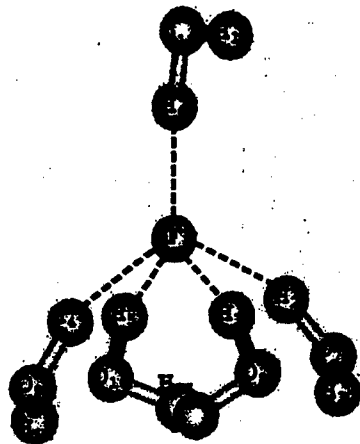
$C_2(C_{2h})$

F1-H2	1.533(1.519)
H2-O4	1.014(1.019)
O4-H6	0.963(0.964)
F1-H2-O4	173.2(173.2)
H2-O4-H6	102.3(102.7)
$\omega$ (F1-H2-O4-H6)	-6.6( 0.0)



$C_3$

F1-H2	1.649(1.603)
H2-O5	0.995(1.003)
O5-H8	0.965(0.965)
H2-F1-H3	88.4( 99.0)
F1-H2-O5	163.8(169.9)
H2-O5-H8	101.2(102.4)
$\omega$ (F1-H2-O5-H8)	34.1( 26.1)



$C_1$

F1-H2	1.855(1.880)
F1-H3	1.751(1.757)
F1-H4	1.872(1.881)
F1-H5	1.787(1.806)
F1-H6	1.685(1.664)
H2-O7	0.978(0.980)
H3-O8	0.983(0.986)
H4-O9	0.978(0.980)
H5-O10	0.982(0.984)
H6-O11	0.988(0.993)
O7-H12	0.969(0.972)
O8-H13	0.968(0.970)
O9-H14	0.969(0.972)
O10-H15	0.968(0.971)
O11-H16	0.963(0.964)
H2-F1-H6	118.5(119.7)
H3-F1-H6	115.7(117.9)
H4-F1-H6	119.5(119.6)
H5-F1-H6	131.5(127.8)
H2-F1-H4	121.4(120.5)
H3-F1-H5	112.8(114.3)
H2-O7-H12	100.8(100.9)
H3-O8-H13	101.1(101.1)
H4-O9-H14	100.7(100.8)
H5-O10-H15	101.1(101.1)
H6-O11-H16	103.0(103.6)

$\omega$ (H2-F1-H6-H4) -171.1  
(-174.5)

$\omega$ (H3-F1-H6-H5) 179.7  
(-179.7)

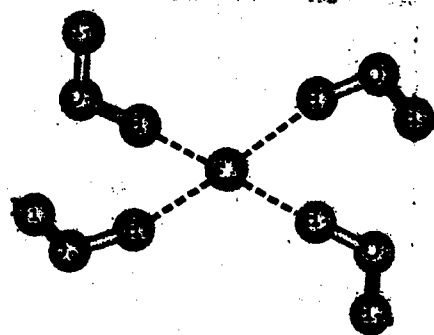
$\omega$ (F1-H2-O7-H12) -38.8  
(-38.6)

$\omega$ (F1-H3-O8-H13) -50.0  
(-44.4)

$\omega$ (F1-H4-O9-H14) -40.8  
(-40.1)

$\omega$ (F1-H5-O10-H15) -48.3  
(-44.4)

$\omega$ (F1-H6-O11-H16) 0.8  
(0.8)



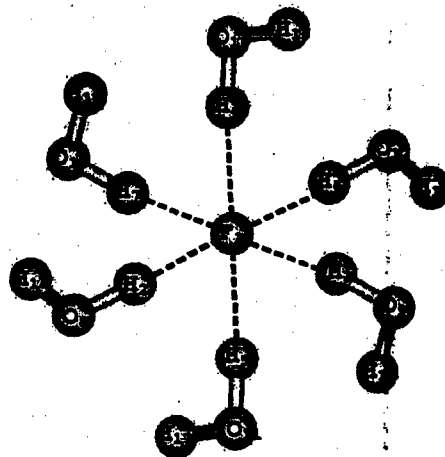
$C_2$

F1-H2	1.618(1.613)
F1-H4	1.786(1.776)
H2-O6	0.996(1.000)
H4-O8	0.982(0.985)
O6-H10	0.963(0.964)
O8-H12	0.967(0.969)
H2-F1-H3	125.2(126.4)
H2-F1-H4	81.6( 82.7)
F1-H2-O6	170.7(169.9)
F1-H4-O8	159.3(159.0)
H2-O6-H10	103.6(103.9)
H4-O8-H12	100.5(100.8)

$\omega$ (H2-F1-H3-H4) -105.0  
(-106.7)

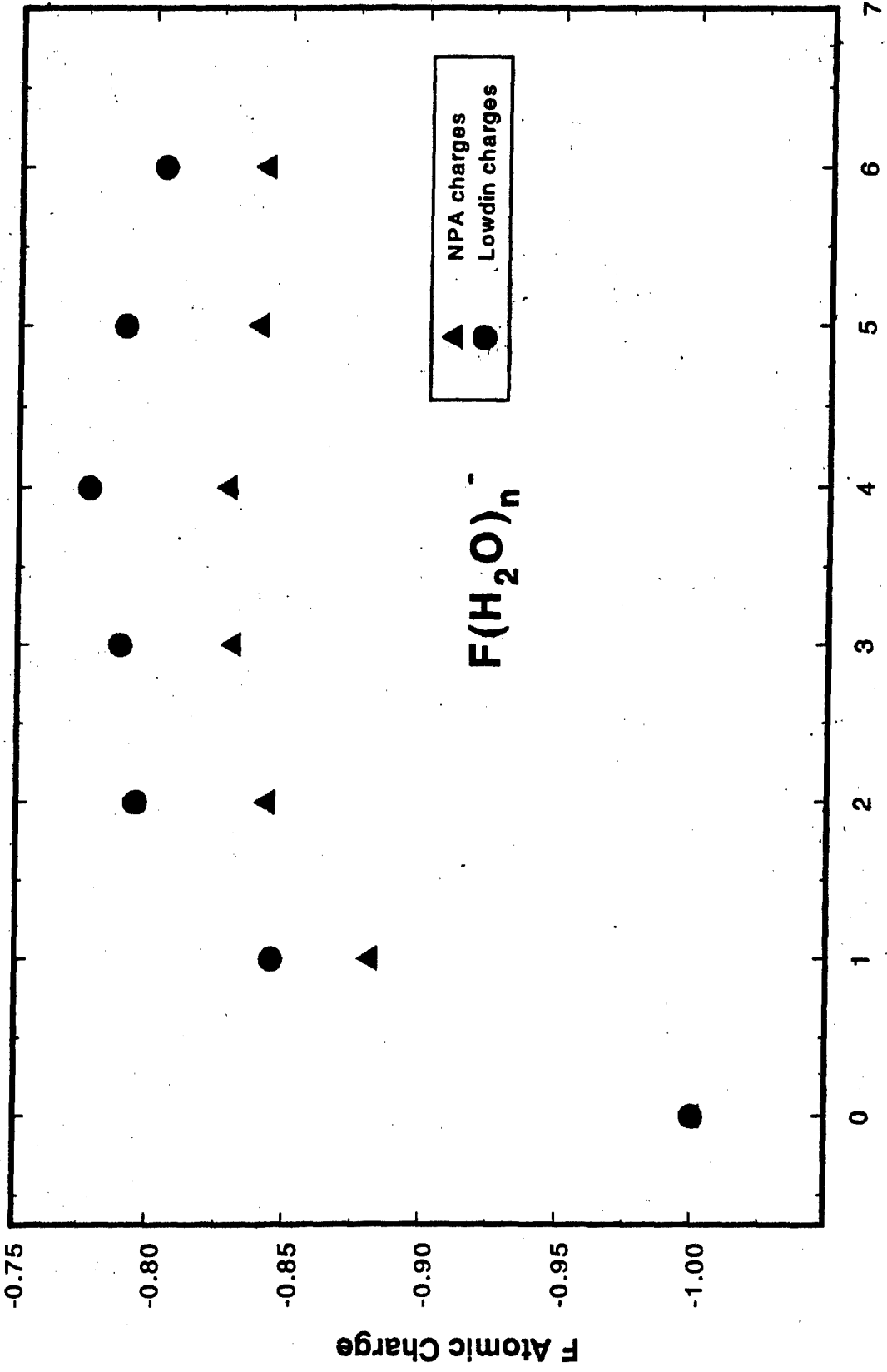
$\omega$ (F1-H2-O6-H10) 80.3  
(74.5)

$\omega$ (F1-H4-O8-H12) -3.3  
(-1.6)

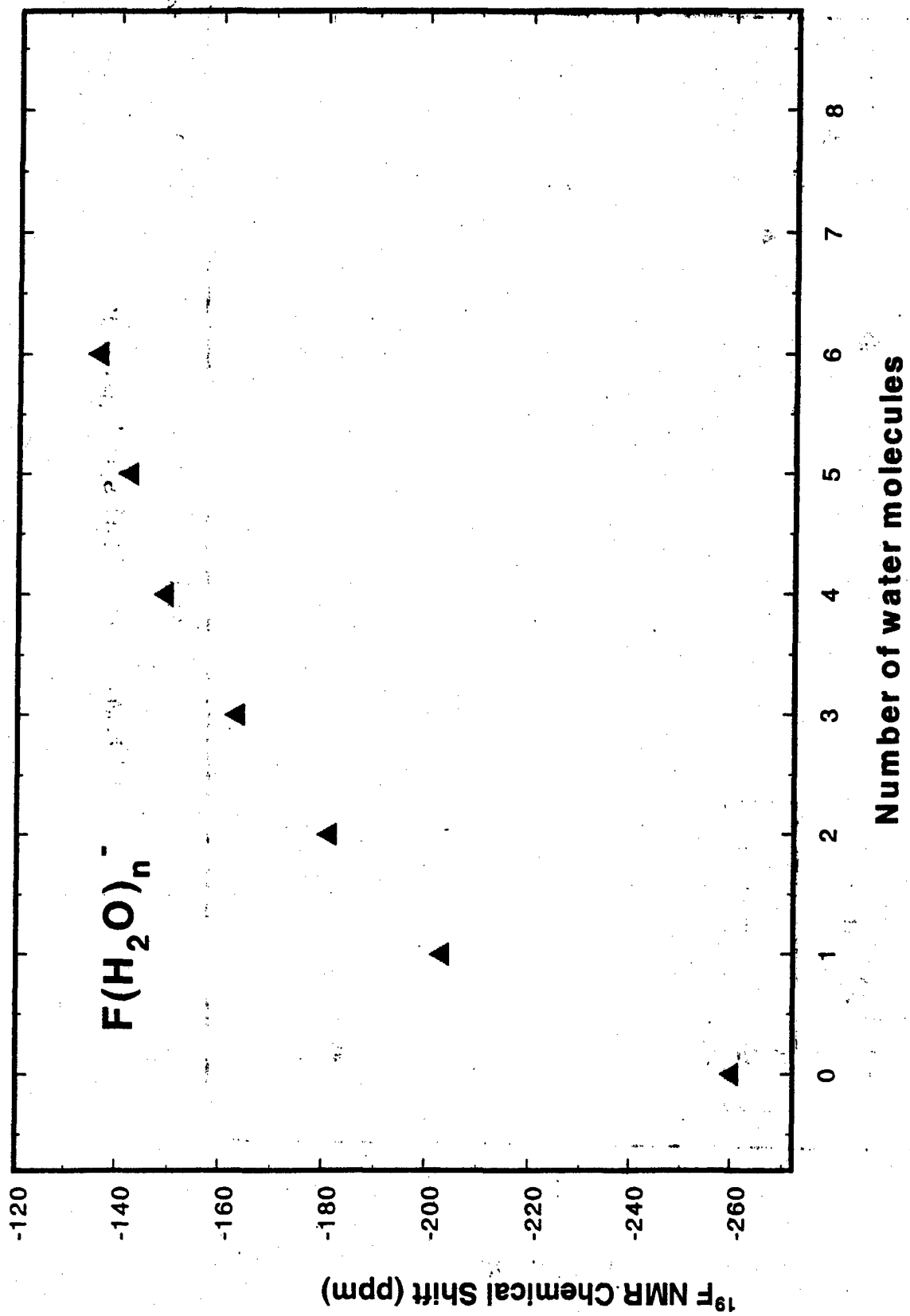


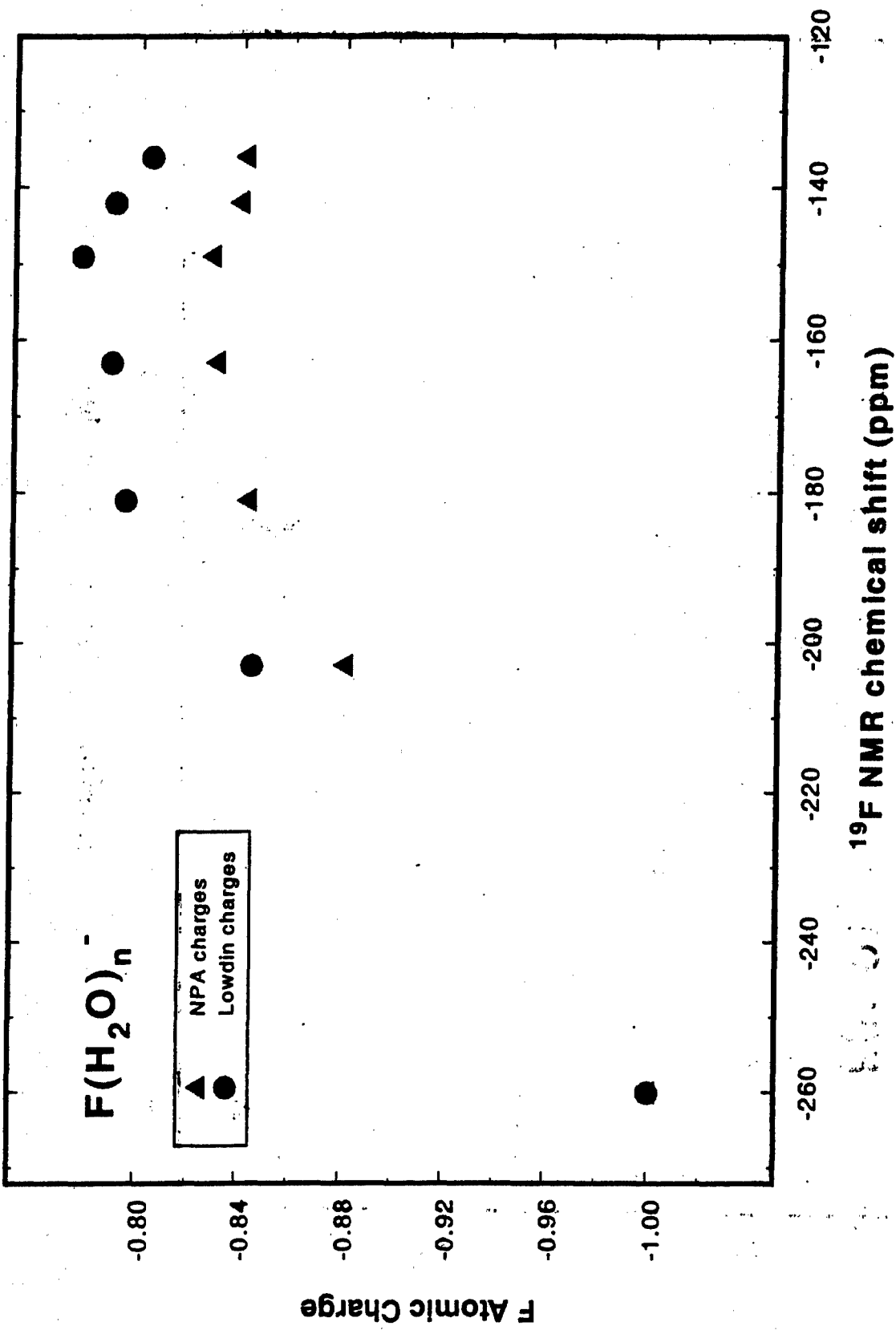
$S_6$

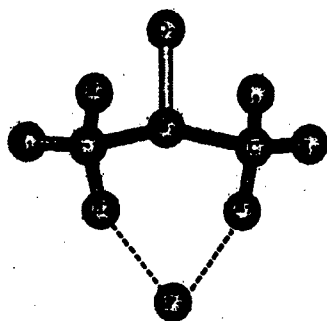
F1-H2	1.821(1.819)
H2-O8	0.978(0.980)
O8-H9	0.967(0.969)
H2-O8-H14	101.5(101.8)
H2-F1-H3	102.7(102.2)
H2-F1-H5	77.3( 77.8)
$\omega$ (F1-H2-O8-H14)	-50.6(-49.0)



Number of water molecules

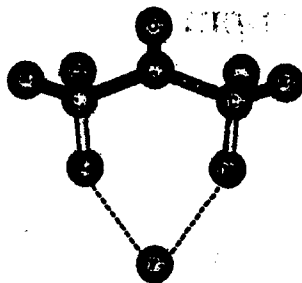






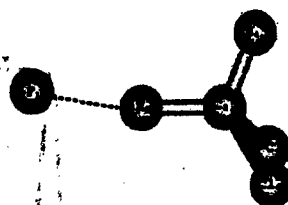
Cs

F3-H6	1.876
S1-O2	1.545
S1-C4	1.797
C4-H6	1.105
C4-H8	1.092
C4-H10	1.089
F3-H6-C4	152.3
H6-F3-H7	74.6
O2-S1-C4	108.1
S1-C4-H6	105.8
S1-C4-H8	107.7
S1-C4-H10	107.7
$\tau(O2-S1-C4-C5)$	62.4
$\omega(F3-H6-H7-S1)$	145.7



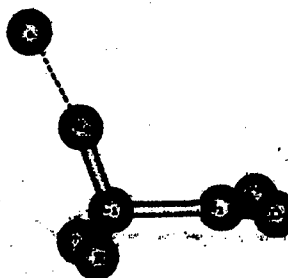
Cs

F3-H6	1.962
C1-O2	1.241
C1-C4	1.503
C4-H6	1.104
C4-H8	1.094
C4-H10	1.089
F3-H6-C4	149.0
H6-F3-H7	72.5
O2-C1-C4	122.7
C1-C4-H6	106.6
C1-C4-H8	109.3
C1-C4-H10	110.3
$\tau(O2-C1-C4-C5)$	-1.9
$\omega(F3-H6-H7-C1)$	164.1



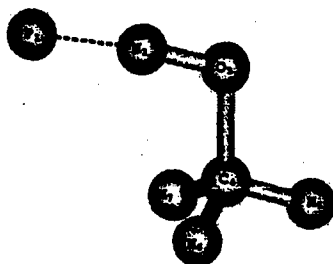
Cs

F1-H2	1.544
H2-C3	1.137
C3-H4	1.085
C3-C15	1.791
F1-H2-C3	171.4
H2-C3-H4	112.2
H2-C3-C15	110.6
H4-C3-C15	106.1
C15-C3-C16	110.6
$\omega(F1-H2-C3-H4)$	0.0



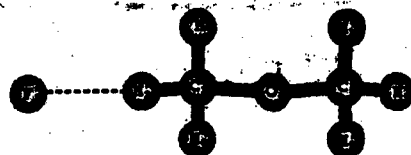
Cs

F8-H5	1.449
H5-C1	1.179
H6-C1	1.086
C1-N2	1.464
N2-O3	1.252
F8-H5-C1	172.3
H5-C1-N2	110.7
C6-C1-N2	106.8
C1-N2-O3	118.6
H6-C1-H7	112.7
$\omega(F8-H5-C1-N2)$	180.0
$\omega(H5-C1-N2-O3)$	88.6



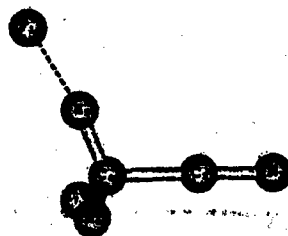
Cs

F1-H2	1.374
H2-O3	1.060
O3-C4	1.400
C4-H5	1.097
C4-H6	1.100
F1-H2-O3	175.2
H2-O3-C4	106.4
O3-C4-H5	109.3
O3-C4-H6	112.6
H5-C4-H6	107.6
$\omega(F1-H2-O3-C4)$	0.0



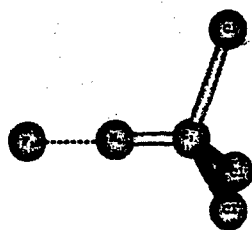
Cs

F1-H2	1.875
H2-C3	1.100
C3-O4	1.441
O4-C5	1.406
C5-H6	1.090
C5-H9	1.099
C3-H7	1.097
F1-H2-C3	158.0
H2-C3-O4	111.0
C3-O4-C5	111.1
O4-C5-H6	107.8
H2-C3-H7	109.6
H7-C3-O4	109.0
O4-C5-H9	111.8
H9-C5-H6	109.0
$\omega(F1-H2-C3-O4)$	180.0



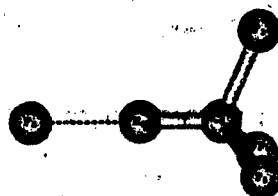
Cs

F1-H5	1.571
H5-C4	1.146
C2-C4	1.457
C2-N3	1.184
C4-H6	1.091
F1-H5-C4	171.5
H5-C4-C2	113.5
C4-C2-N3	180.0
H5-C4-H6	108.6
H6-C4-H7	108.7
$\omega(F1-H5-C4-C2)$	180.0



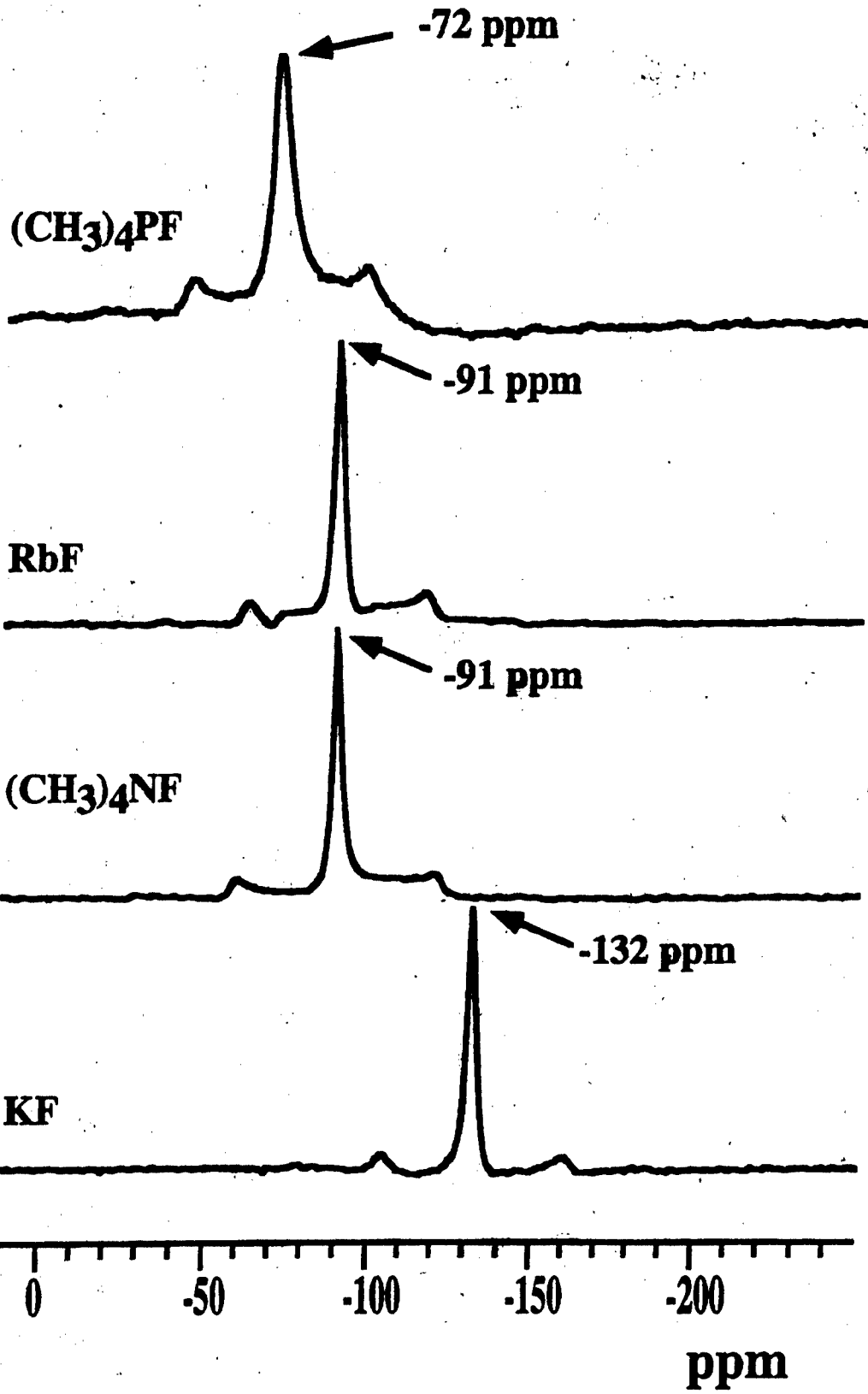
C3v

F2-H1	1.377
H1-C3	1.189
C3-C14	1.788
H1-C3-C14	110.1
C14-C3-C15	108.8



C3v

F6-H2	1.536
H2-C1	1.133
C1-F3	1.376
H2-C1-F3	113.3
F3-C1-F4	105.3



## Are $^{19}\text{F}$ NMR shifts a measure for the nakedness of fluoride ions?

M. Gerken<sup>a</sup>, A. Boatz<sup>b</sup>, A. Kornath<sup>a</sup>, R. Haiges<sup>a</sup>, S. Schneider<sup>a</sup>, T. Schroer<sup>a</sup>,  
K. O. Christe<sup>a,b\*</sup>

<sup>a</sup>Loker Hydrocarbon Research Institute, University of Southern California, Los Angeles, CA 90089, USA  
<sup>b</sup>Air Force Research Laboratory, Edwards AFB, CA 93524, USA

Fluoride ions in either solution or the solid state exhibit a wide range of  $^{19}\text{F}$  NMR shifts due to paramagnetic contributions from solvent interactions or ion-ion overlap. The only truly "naked" fluoride is the free gaseous ion. The MAS  $^{19}\text{F}$  NMR spectra of  $\text{N}(\text{CH}_3)_4\text{F}$  and  $\text{P}(\text{CH}_3)_4\text{F}$  are reported and exhibit  $^{19}\text{F}$  chemical shifts of  $-91$  and  $-72$  ppm, respectively. The stepwise build-up of a sphere and the electron charge transfer from  $\text{F}^-$  to  $\text{H}_2\text{O}$  were modeled for the  $\text{F}^-/\text{H}_2\text{O}$  system. The minimum energy structures of the 1:1 adducts of  $\text{F}^-$  with  $\text{CH}_3\text{OH}$ ,  $\text{H}_2\text{O}$ ,  $\text{CH}_3\text{OCH}_3$ ,  $\text{CHCl}_3$ ,  $\text{CH}_2\text{Cl}_2$ ,  $\text{CHF}_3$ ,  $\text{CH}_3\text{CN}$ ,  $\text{CH}_3\text{NO}_2$ ,  $(\text{CH}_3)_2\text{SO}$ , and  $\text{CH}_3\text{COCH}_3$  were calculated, and the calculated  $^{19}\text{F}$  NMR shift trends agree with the observed ones.

